Elsevier Editorial System(tm) for Energy Conversion and Management

Manuscript Draft

Manuscript Number: ECM-D-18-03229

Title: Exergy Analysis and Optimization of a Combined Cooling and Power System Driven by Geothermal Energy for Ice-making and Hydrogen Production

Article Type: Original research paper

Section/Category: 1. Energy Conservation and Efficient Utilization

Keywords: Geothermal, Jaya algorithm, Hydrogen production, ice production

Corresponding Author: Dr. Jiangfeng Wang, Ph.D.

Corresponding Author's Institution: Xi'an Jiaotong University

First Author: Liyan Cao

Order of Authors: Liyan Cao; Juwei Lou; Jiangfeng Wang, Ph.D.; Yiping Dai

Abstract: This paper investigates a combined cooling and power system driven by geothermal energy for ice-making and hydrogen production. The proposed system combines geothermal flash cycle, Kalina cycle, ammonia-water absorption refrigeration cycle and electrolyser. The geothermal energy can be efficiently converted to storable hydrogen and ice. Based on mathematical model, some key parameters are analyzed to figure out their effect on the exergetic performance. An exergy destruction for all components has been performed to find out the distribution of exergy inefficiency. The system exergetic efficiency is optimized by Jaya algorithm and Genetic algorithm and the optimization results are compared. According to the parametric analysis, the exergy efficiency decreases as the back pressure of steam turbine and the back pressure of ammonia-water turbine increase. The exergy efficiency could increase first and then decline, as flash pressure, ammonia-water turbine inlet pressure and ammonia mass fraction of basic solution increase. The optimization results show that the exergy efficiency reaches 23.59%, 25.06% and 26.25% when the geothermal water temperature is 150℃, 160℃ and 170℃. Jaya algorithm has highly precise optimization results.

Suggested Reviewers: Zhixin Sun
Fuzhou University, PR China
zxsun@fzu.edu.cn
Experienced scholar in energy system and hydrogen production

Weifeng He
Nanjing University of Aeronautics & Astronautics, PR China
heweifeng_turbine@163.com
He specializes in low-grade heat recovery.

Pouria Ahmadi
University of Ontario Institute of Technology, Canada
Pouria.Ahmadi@uoit.ca

Dear Editor:

We are sending a manuscript entitled "***Exergy Analysis and Optimization of a Combined Cooling and Power System Driven by Geothermal Energy for Ice-making and Hydrogen Production***", which we should like to submit for publication in ***Energy Conversion and Management***. We investigated a combined cooling and power system driven by geothermal energy for ice-making and hydrogen production. The mathematical model of the system is established to simulate the cycles under steady-state conditions. A parametric analysis of some key parameters is conducted to examine their effects on the system performance. An optimization is conducted by a novel optimization algorithm named Jaya algorithm and Genetic algorithm to obtain the maximum exergy efficiency.

We declare that the manuscript has not been previously published, is not currently submitted for review to any other journal and will not be submitted elsewhere before one decision is made. Its publication is approved by all authors. If accepted, it will not be published elsewhere in the same form, in English or in any other language.

We appreciate your consideration of our manuscript, and we look forward to receiving comments from the reviewers.

Sincerely,

Jiangfeng Wang (on behalf of the authors' team)

Institute of Turbomachinery

Shaanxi Engineering Laboratory of Turbomachinery and Power Equipment

State Key Laboratory of Multiphase Flow in Power Engineering

School of Energy and Power Engineering

Xi'an Jiaotong University, Xi'an, China

Highlights

- A combined cooling and power system driven by geothermal energy for ice-making and hydrogen production are proposed.
- The effects of parameters on system performance are examined.
- Optimizations for a combined cooling and power system for ice-making and hydrogen production are conducted by Jaya algorithm and Genetic algorithm.

Exergy Analysis and Optimization of a Combined Cooling and Power System Driven by Geothermal Energy for Ice-making and Hydrogen Production

Liyan Cao, Juwei Lou, Jiangfeng Wang*, Yiping Dai

Institute of Turbomachinery, Shaanxi Engineering Laboratory of Turbomachinery and Power Equipment, State Key Laboratory of Multiphase Flow in Power Engineering, School of Energy and Power Engineering, Xi'an Jiaotong University, Xi'an 710049, China

Corresponding author: Jiangfeng Wang.

Mailing address:

Institute of Turbomachinery, Shaanxi Engineering Laboratory of Turbomachinery and Power Equipment, State Key Laboratory of Multiphase Flow in Power Engineering, School of Energy and Power Engineering

Xi'an Jiaotong University, Xi'an 710049, China

E-mail address: jfwang@mail.xjtu.edu.cn (JF Wang).

Exergy Analysis and Optimization of a Combined Cooling and Power System Driven by Geothermal Energy for Ice-making and Hydrogen Production

Liyan Cao, Juwei Lou, Jiangfeng Wang*, Yiping Dai

Institute of Turbomachinery, Shaanxi Engineering Laboratory of Turbomachinery and Power Equipment, State Key Laboratory of Multiphase Flow in Power Engineering, School of Energy and Power Engineering, Xi'an Jiaotong University, Xi'an 710049, China

Abstract

This paper investigates a combined cooling and power system driven by geothermal energy for ice-making and hydrogen production. The proposed system combines geothermal flash cycle, Kalina cycle, ammonia-water absorption refrigeration cycle and electrolyser. The geothermal energy can be efficiently converted to storable hydrogen and ice. Based on mathematical model, some key parameters are analyzed to figure out their effect on the exergetic performance. An exergy destruction for all components has been performed to find out the distribution of exergy inefficiency. The system exergetic efficiency is optimized by Jaya algorithm and Genetic algorithm and the optimization results are compared. According to the parametric analysis, the exergy efficiency decreases as the back pressure of steam turbine and the back pressure of ammonia-water turbine increase. The exergy efficiency could increase first and then decline, as flash pressure, ammonia-water turbine inlet pressure and ammonia mass fraction of basic solution increase. The optimization results show that the exergy efficiency reaches 23.59%, 25.06% and 26.25% when the geothermal water temperature is 150℃, 160℃ and 170℃. Jaya algorithm has highly precise optimization results.

Key words: Geothermal, Jaya algorithm, Hydrogen production, ice production

Nomenclature

c_p	specific heat capacity, kJ/(kg K)
E	exergy, kW
HHV	higher heating value, kJ/mol
h	specific enthalpy, kJ/kg
I	exergy destruction, kW
M	molecular weight, g/mol
m	mass flow rate, kg/s
Q	energy, kW
s	specific entropy, kJ/(kg K)
T	temperature, K
t	temperature, ℃
V	volumetric flow rate, L/s
VG	vapor generator
W	power, kW
x	ammonia mass fraction, %
Greek letters	
ρ	density, kg/m^3
η	efficiency, %
Subscript	
amb	ambient
awt	ammonia-water turbine

basic	ammonia-water basic solution
elec	electrolyser
exg	exergy
gen	generating
geo	geothermal water
H_2	hydrogen
ice	ice
in	inlet
l	liquid
mech	mechanical
motor	motor
net	net
poor	ammonia-poor solution
poor2	secondary ammonia-poor solution
pump	pump
ref	refrigeration
rich	ammonia-rich vapor
rich2	secondary ammonia-rich vapor
s	isentropic
st	steam turbine
v	vapor
1-28	state point

1. Introduction

In recent years, the demand for fossil fuels increases dramatically, which has aroused great concerns about the environmental pollution, greenhouse gas emission and security of energy supply. Different countries have set out a plan to achieve diversification of energy supply and increase the proportion of renewable energy. Geothermal energy is one of the most reliable, sustainable and environmentally friendly renewable energy. Variety of schemes have been proposed to achieve efficient and cost-effective utilization of Geothermal energy.

Worldwide, geothermal power generation is the most common and efficient method for geothermal utilization. Geothermal power generation technologies in use mainly include flash cycle, binary cycle and flash-binary cycle. Researchers conducted analysis and optimization of the flash cycle [1-3]. But the flash cycle requires a relatively high geothermal water temperature. For the geothermal well with low water temperature, Kalina cycle [4-7] is regarded as reliable technologies, since Kalina cycle take full advantage of ammonia-water mixture. Owing to its low-boiling point and temperature slide character, ammonia-water mixture can achieve better thermal match in evaporator to reduce the irreversible loss. On this basis, Kalina cycle has applied as the bottom cycle of flash cycle to raise the thermal and exergy efficiency [8, 9]. However, the traditional Kalina cycle or flash-Kalina cycle only generate power, which cannot satisfy the diversified energy demand of users.

The cogeneration systems can supply users with different kinds of energy including electricity, heat and cooling, but more importantly, it has higher energy efficiency. From thermodynamic point of view, cooling is not an easily accessible form of energy

compared to heat. It is usually converted from heat or electricity. Therefore, this brings a focus on the combined power and cooling (CCP) system employing ammonia–water as working fluid. Goswami and Xu [10, 11] came up with a combined cooling and power cycle based on ammonia-water absorption refrigeration cycle. They claimed that this cycle had potential for efficient recovery of low-grade heat source. Demirkaya *et al.* [12] conducted parametric analysis of Goswami cycle and examined the effect of operation and configuration parameters, including the number of turbine stages and different superheating configurations, on the cycle performance. They found multiple stage turbines had a better performance than single stage turbines did. It is also on the basis of the ammonia-water absorption refrigeration cycle, Mendoze *et al*. [13] proposed another combined cooling and power cycle. The ammonia vapor from rectifier was split into two streams that were used to generate cooling in the evaporator and to drive turbine to produce power, respectively. Ghaebi [14] came up with a new combined cooling and power (CCP) cycle, using geothermal energy as low-temperature heat source. The proposed cycle was integrated from a Kalina cycle and an ejector refrigeration cycle to produce refrigeration and power outputs simultaneously. Han *et al*. [15] experimental investigation on a combined refrigeration/power generation system. The net power output and cooling output were 1.02kW and 11.67 kW.

However, the energy demand of users may periodically fluctuate with time. This will trigger the mismatch between energy supply and demand. At lower load of energy demand, the operation condition of CCP system can be adjusted to meet the change of energy demand, but it will deviate from the design condition and go against the efficient operation of the CCP system. To solve this problem, some researchers try to store

electricity energy into hydrogen energy to eliminate the mismatch. Yüksel [16] conducted thermodynamic analysis for a combined cooling, power and hydrogen production system driven by solar energy. The high temperature water from solar collector drove an Organic rankine cycle and an absorption cooling system to produce electricity and cooling, respectively. A part of electricity was used for hydrogen production by a Proton Exchange Membrane (PEM) electrolyser. Khanmohammadi *et al*. [17] proposed a similar combined cooling, power and hydrogen production system and carried out a parametric study to determine the main design parameters and their effects on the objective functions of the system. Akrami *et al*. [18] proposed multi-generation system comprised of a geothermal based organic Rankine cycle, domestic water heater, absorption refrigeration cycle and PEM electrolyser. The geothermal water was used to boost ORC and to heat the domestic water up, successively. A part of power generated by organic turbine was used for hydrogen production and organic turbine exhaust was regarded as the heat source of absorption refrigeration cycle. Yuksel *et al.* [19] came up with a novel integrated geothermal energy-based system for cooling and hydrogen production. The cooling and hydrogen was produced by an absorption refrigeration cycle and PEM electrolyser, separately. They claimed that the energetic and exergetic efficiencies of the integrated system could reach to 42.59% and 48.24%, respectively. Parham *et al*. [20] proposed a novel multi-generation system including an open absorption heat transformer an ORC and an electrolyser for hydrogen production. They analyzed the system from both first and second laws of thermodynamics.

As was summarized above, all the combined cooling, power and hydrogen systems could convert electricity to hydrogen that can be easily stored to counter the mismatch

between supply and demand. However, these papers don't take the cooling mismatch into consideration. In addition, all the systems generate electricity and cooling with separate cycles, and different cycles run with different working medium. As a result, the systems have very complex configurations. We believe that the cogeneration system could have a more compact configuration and all the products are storable. Toward this end, in this paper, we propose a combined cooling and power system driven by geothermal energy for ice-making and hydrogen production. The system consists of a top geothermal flash cycle, a bottom combined cooling and power cycle as well as an electrolyser. For the bottom cycle, both Kalina cycle and absorption refrigeration cycle can adopt ammonia-water as working fluid, we integrate Kalina cycle with absorption refrigeration cycle by sharing same key components to simplify the system configuration. And electricity and cooling are converted to storable hydrogen and ice, respectively. We also conduct a parametric analysis to study the effect of key parameters on system performance. In addition, we use a novel optimization algorithm named Jaya algorithm to optimize the systems and compare the Jaya algorithm with Genetic algorithm to verify its accuracy.

2. System description

Fig. 1 shows the schematic diagram of a combined cooling and power system for ice-making and hydrogen production. The high-temperature geothermal water is pumped from geothermal well to flashing devise in which the geothermal water is decompressed and partially becomes steam. The steam expands in steam turbine and the exhaust leaves turbine with low temperature and low pressure. The remaining water from flashing devise is used to vaporize the ammonia-water basic solution in vapor generator (VG), and then the water is mixed with steam turbine exhaust and delivered to recharge well. The

vaporized ammonia-water basic solution is delivered to separator 1, in which it is separated into ammonia-rich vapor and ammonia-poor solution. After expanding in ammonia-water turbine to generate electrical power, the ammonia-water turbine exhaust is separated into secondary ammonia-rich vapor and secondary ammonia-poor solution in separator 2. The secondary ammonia-rich vapor is condensed and throttled down to generate cold energy in evaporator. The generated cold energy is used to produce ice. The secondary ammonia-poor solution from separator 2, the secondary ammonia-rich vapor from evaporator and the ammonia-poor solution from separator 1 are mixed and condensed into supercooling ammonia-water basic solution in condenser 2. The ammonia-water basic solution is preheated in regenerator 1 and regenerator 2. Finally, the ammonia-water basic solution is delivered to VG to complete the bottom cycle. All the power generated by turbines is given to electrolyser to break the molecules of water into hydrogen and oxygen.

3. Mathematical model and performance criteria

The mathematical model is established based on mass and energy conservation. For the sake of simplification of the mathematical model, some assumptions are applied as follows:

(1) The system is simulated in steady state.

(2) The flows across the throttle valve are isenthalpic.

(3) The working fluid is condensed to saturated liquid in condenser.

(4) The pressure loss and heat loss are neglected.

(5) Turbines and pumps have isentropic efficiency.

3.1 Mathematical model

For the flashing devise, the mass and energy balance equations are described as:

$$\frac{m_{\mathrm{v}}}{m_{\mathrm{geo}}} = \frac{h_1 - h_3}{h_2 - h_3} \tag{1}$$

$$m_{\mathrm{geo}} = m_l + m_{\mathrm{v}} \tag{2}$$

For the VG, energy balance equation is expressed as:

$$m_{\mathrm{l}}(h_3 - h_4) = m_{\mathrm{basic}}(h_7 - h_9) \tag{3}$$

For the steam turbine, the isentropic expansion efficiency is represented as:

$$s_2 = s_{5\mathrm{s}} \tag{4}$$

$$\eta_{\mathrm{st}} = \frac{h_2 - h_5}{h_2 - h_{5\mathrm{s}}} \tag{5}$$

For the separator 1, the mass and energy balance equation are written as:

$$m_{\mathrm{basic}} = m_{\mathrm{rich}} + m_{\mathrm{poor}} \tag{6}$$

$$m_{\mathrm{basic}} x_7 = m_{\mathrm{rich}} x_8 + m_{\mathrm{poor}} x_9 \tag{7}$$

$$m_{\mathrm{basic}} h_7 = m_{\mathrm{rich}} h_8 + m_{\mathrm{poor}} h_9 \tag{8}$$

For the ammonia-water turbine, isentropic expansion efficiency can be expressed as:

$$s_8 = s_{10\mathrm{s}} \tag{9}$$

$$\eta_{\mathrm{awt}} = \frac{h_8 - h_{10}}{h_8 - h_{10\mathrm{s}}} \tag{10}$$

For the evaporator, the energy balance equation is given by:

$$m_{\mathrm{rich2}}(h_{17} - h_{16}) = m_{\mathrm{water}}(h_{23} - h_{24}) \tag{11}$$

For the heat regenerator 1, the energy balance equation is defined as:

$$m_{\mathrm{basic}}(h_{20} - h_{19}) = m_{\mathrm{v}}(h_5 - h_6) \tag{12}$$

For the heat regenerator 2, the energy balance equation is described as follows:

$$m_{\text{basic}}(h_{25}-h_{20})=m_{\text{poor2}}(h_9-h_{13}) \tag{13}$$

For the evaporator, the mass and energy balance equations is as follows:

$$m_{\text{rich}}=m_{\text{rich2}}+m_{\text{poor2}} \tag{14}$$

$$m_{\text{rich}}h_{10}=m_{\text{rich2}}h_{11}+m_{\text{poor2}}h_{12} \tag{15}$$

The isenthalpic flow across the throttle valves has the form:

$$h_{13}=h_{14} \tag{16}$$

$$h_{15}=h_{16} \tag{17}$$

$$h_{12}=h_{26} \tag{18}$$

The power consumption and isentropic efficiency of pumps are defined as:

$$\eta_{\text{pump}}=\frac{h_{19\text{s}}-h_{18}}{h_{19}-h_{18}} \tag{19}$$

$$\eta_{\text{pump}}=\frac{h_{22\text{s}}-h_{21}}{h_{22}-h_{21}} \tag{20}$$

$$W_{\text{pump}}=(h_{19}-h_{18})m_{\text{basic}}+(h_{22}-h_{21})m_{\text{v}} \tag{21}$$

The electric power generated by turbine is given by:

$$W_{\text{st}}=m_{\text{v}}(h_2-h_5) \tag{22}$$

$$W_{\text{awt}}=\left[m_{\text{rich}}(h_8-h_{10})\right] \tag{23}$$

$$W_{\text{net}}=\left(W_{\text{st}}+W_{\text{awt}}\right)\eta_{\text{mech}}\eta_{\text{gen}}-W_{\text{pump}}/\eta_{\text{pump,motor}} \tag{24}$$

where η_{mech}, η_{gen} and $\eta_{\text{pump,motor}}$ are mechanical efficiency, generator efficiency and pump motor efficiency, respectively.

In this paper, all the power is used to produce hydrogen by electrolysis of water. The

198 Higher Heating Value (*HHV*) of hydrogen is 285.840 kJ/mol. That's to say, burning one
199 mold of hydrogen would produce one mole of water and release 285.840kJ of heat.
200 Ideally, electrolyzing one mole of water to produce one mole of hydrogen will consumes
201 285.840kJ of heat [21].

202 $$4H_2O+4e^- = 2H_2 \uparrow +4OH^- \quad (25)$$

203 $$4OH^- -4e^- = 2H_2O+O_2 \uparrow \quad (26)$$

204 In this paper, an alkaline electrolyser is chosen to produce hydrogen. The total
205 efficiency of the electrolyser is 77%, which has taken energy dissipations of AC/DC
206 converter and other equipment into consideration [21]. The hydrogen production is given
207 by

208 $$V_{H_2} = \frac{W_{net} \cdot 1000 \cdot M_{H_2} \cdot \eta_{elec}}{HHV \cdot V_{H_2} \cdot \rho_{H_2}} \quad (27)$$

209 where V_{H_2}, M_{H_2}, ρ_{H_2} and η_{elec} are volumetric flow rate of hydrogen, molecular weight
210 of hydrogen, density of hydrogen and efficiency of the electrolyser, respectively.

211 The cold energy generated by evaporator to make ice is defined as:

212 $$Q_{ref} = m_{ice} c_p (T_{23} - T_{24}) \quad (28)$$

213 where m_{ice} is the ice production rate.

214 **3.2 Performance criteria**

215 The thermodynamic performance of system is evaluated by system exergy efficiency
216 and hydrogen exergy efficiency. The exergy is given by:

217 $$E = (h - h_{amb}) - T_{amb}(s - s_{amb}) \quad (29)$$

218 The cold exergy is written as:

219 $$E_{ref} = T_{amb}(s - s_{amb}) - (h - h_{amb}) \quad (30)$$

The exergy of hydrogen approximately equals to the HHV of H_2, namely 285.840 kJ/mol [21].

The system exergy efficiency is expressed as:

$$\eta_{\text{exg}} = \frac{E_{\text{H}_2} + E_{\text{ref}}}{E_{\text{in}}} \tag{31}$$

The hydrogen efficiency is expressed as:

$$\eta_{\text{exg-H}_2} = \frac{E_{\text{H}_2}}{E_{\text{in}}} \tag{32}$$

E_{in} is the exergy input defined as:

$$E_{\text{in}} = m_{\text{geo}} E_1 - m_l E_4 - m_{\text{v}} E_{22} \tag{33}$$

The exergy destruction is defined as follows.

$$I = \Delta_{\text{out}}^{\text{in}} E \tag{34}$$

4. Results and discussion

In this section, a parametric analysis for the combined cooling and power system for ice-making and hydrogen production is performed. Some key parameters (e.g. flash pressure, ammonia mass fraction of basic solution, ammonia-water turbine inlet pressure, ammonia-water turbine back pressure, steam turbine back pressure) are analyzed to figure out their effect on the system performance. The thermodynamic properties of working fluid are calculated by REFPROP 9.1 developed by the National Institute of Standard and Technology (NIST) of the United States. The simulation of the system is conducted by MATLAB software. The simulation boundary condition and simulation results are listed in Table 1 and Table 2. Fig. 2 illustrates the exergy destruction distribution of critical components under simulation condition.

Fig. 2 shows the exergy destruction of different components. The largest exergy destruction takes place in condensers, which is mainly caused by large heat transfer temperature differences. The exergy destruction of steam turbine and ammonia-water turbine are 15.99%. Heat regenerators contribute 14.72% of total exergy destruction. For VG & evaporator, valves, separators and other components, the exergy destruction are 7.89%, 7.04%, 5.56% and 7.11%, respectively.

4.1 Parametric analysis

Fig. 3 shows the effect of flash pressure on system performance. As the flash pressure increases, the mass flow rate of steam decreases, leading to a decrease in the power output of steam turbine. Meanwhile, the mass flow rate of water from flashing device increases with flash pressure. The mass flow rate of ammonia-rich vapor increases, and the power output of ammonia-water turbine increases as well. Under the comprehensive impact of steam turbine and ammonia-water turbine, the net power output of the system firstly increases and then decreases. Thus, the hydrogen production has the same variation when the flash pressure increases. The increment of the mass flow rate of secondary ammonia-rich vapor results in the increase in refrigeration exergy. Therefore, the ice production increases. Since, the hydrogen production increases firstly and the decreases, the variation of hydrogen exergy efficiency shows a convex curve. For system exergy efficiency, the refrigeration exergy is much smaller than the hydrogen exergy. Hence, the impact of refrigeration exergy on system exergy efficiency is negligible. The variation of system exergy efficiency shows a convex curve as well.

Fig. 4 shows the effect of steam turbine back pressure on the system performance. Since the bottom cycle is independent of the steam turbine back pressure, the power

output of ammonia-water turbine, the refrigeration exergy and ice production won't change with variation of the steam turbine back pressure. Meanwhile, the increment of steam turbine back pressure causes a decrease in power output of steam turbine. Consequently, the decreasing net power output of the system results in the decreasing hydrogen production of the system. The hydrogen exergy efficiency and system exergy efficiency decrease as well.

Fig. 5 shows the effect of ammonia mass fraction of basic solution on system performance. When the ammonia mass fraction of basic solution increases, the power output of steam turbine remains unchanged, and the mass flow rate of ammonia-rich vapor and secondary ammonia-rich vapor rise simultaneously, which enables the net power output, the hydrogen production, the refrigeration exergy and ice production increase. Meanwhile, the energy and exergy input increase with ammonia mass fraction of basic solution as well. Under the comprehensive impact of increasing exergy input, hydrogen production and refrigeration exergy, the hydrogen exergy efficiency and system exergy efficiency both show the convex curves.

Fig. 6 shows the effect of ammonia-water turbine inlet pressure on system performance. The flash cycle is independent of ammonia-water turbine inlet pressure. Thus, the power output of steam turbine remains unchanged. When the ammonia-water turbine inlet pressure increases, the variation of the specific enthalpy drop in ammonia-water turbine is opposite to that of the mass flow rate of ammonia-rich vapor. Under the impact of these two factors, the net power output of the system as well as the hydrogen production firstly increases and then decreases. In addition, the mass flow rate of secondary ammonia-rich vapor decrease, which causes a decrease in refrigeration exergy

and ice production. Meanwhile, the energy and exergy input decrease when the ammonia-water turbine inlet pressure increases. Under the comprehensive impact, the hydrogen exergy efficiency and system exergy efficiency show convex curves.

Fig. 7 shows the effect of ammonia-water turbine back pressure on system performance. As the ammonia-water turbine back pressure increases, the mass flow rate of ammonia-rich vapor remains unchanged, and the enthalpy drop through ammonia-water turbine decreases. This causes a decrease in power output of ammonia-water turbine. Meanwhile, the power output of steam turbine keeps unchanged. Therefore, the net power output of the system decreases as well, which leads to the decline of hydrogen production. The refrigeration exergy and ice production decrease since the mass flow rate of secondary ammonia-rich solution decreases. The exergy input is independent of ammonia-water turbine back pressure. Thus, the hydrogen exergy efficiency and system exergy efficiency decline, as the ammonia-water turbine back pressure increases.

4.2 Optimization

According to the parametric analysis, there may be an optimum performance for the combined cooling and power system driven by geothermal energy for ice-making and hydrogen production. Thus, a performance optimization is conducted to obtain the maximum system exergy efficiency. There are many optimization methods, such as Genetic algorithm (GA), Teaching-learning-based optimization (TLBO), Evolution Strategy (GE) and Evolution Programming (EP). For the performance optimization of the system driven by law temperature heat source, GA is the most commonly used optimization method for its global optimization ability [22-24].

Recently, Rao and Waghmare [25] proposed a new optimization algorithm named Jaya algorithm (JA) and compared JA with other algorithms. Unlike other algorithms, JA requires only the common control parameters such as population size, number of generations and elite size to run the optimization algorithm. And other algorithms require common control parameters as well as their own algorithm-specific parameters, which could add complexity to the algorithms [25]. The author tested JA and other several optimization algorithms on 21 benchmark problems related to constrained design optimization and claimed that JA could get highly precise optimization results with less computational time. The brief introduction of JA is as follows.

The objective function $f(x)$, which is a function of m design variables (j=1,2,…,m), is to be maximized and minimized by JA. At any i^{th} generation, there are n candidate solutions associated with n populations (k=1,2,…,n). And $x_{j,k,i}$ is the j^{th} variable in k^{th} population at i^{th} generation. The best value and worst value among n candidate solutions at i^{th} generation are $f(x)_{best,i}$ and $f(x)_{worst,i}$. Therefore, $x_{j,best,i}$ is the j^{th} variable in the population that corresponds to the best candidate solution $f(x)_{best,i}$, and $x_{j,worst,i}$ is the j^{th} variable in the population that corresponds to the worst candidate solution $f(x)_{worst,i}$ at i^{th} generation. For $(i+1)^{th}$ generation, x is modified as,

$$x_{j,k,i+1} = x_{j,k,i} + r_{1,j,i}(x_{j,best,i} - |x_{j,k,i}|) - r_{2,j,i}(x_{j,worst,i} - |x_{j,k,i}|) \quad (35)$$

where $r_{1,j,i}$ and $r_{2,j,i}$ both are the random numbers between 0 and 1. The Flow chart of Jaya algorithm is showed in Fig. 8.

To verify the optimization accuracy of JA algorithm, a system performance optimization is conducted by using both JA and GA with the same boundary condition

and common control parameters. It is noted that the system is optimized under three different geothermal water temperatures (150℃, 160℃ and 170℃) to guarantee reliability of comparative results. For each geothermal water temperature, the optimizations with JA and GA are performed with three and five different population size, respectively. The optimization with JA is carried out using the program written in Matlab by authors. The optimization with GA is performed by Matlab optimization tool box. All optimizations are running in the completely same computing environment. The operation parameters of optimization algorithm and ranges of key thermodynamic parameters are listed in Table 3 and the optimization results are listed in Table 4.

Under three different geothermal water temperatures, the optimum exergy efficiencies calculated by JA almost keep constant for different population sizes. The exergy efficiencies are about 23.59%, 25.06% and 26.25% for geothermal water temperature of 150℃, 160℃ and 170℃, respectively. These results almost equal to those calculated by GA when the population sizes are 50 and 100. That's to say, the JA results are acceptably accurate. Meanwhile, we can find that small population size leads to inaccurate GA results; and even if the population size is small, JA could still obtain accurate results. In other words, JA could get accurate results with less population, which has potential to save computational time.

5. Conclusions

In this paper, we propose a combined ice-making and hydrogen production system. We investigate the exergy destruction of different components and analyze the effect of key parameters on system performance. We also conduct an optimization with JA and GA

to search for maximum exergy efficiencies under three different geothermal water temperatures. The main conclusions are as follow:

(1) The condensers contribute most to the exergy destruction owing to the high temperature difference. The exergy efficiency decreases as back pressure of steam turbine and ammonia-water turbine increase. And exergy efficiency shows a convex curve, as flash pressure, ammonia-water turbine inlet pressure and ammonia mass fraction of basic solution increase.

(2) The optimum exergy efficiencies calculated by JA are about 23.59%, 25.06% and 26.25% for geothermal water temperature of 150℃, 160℃ and 170℃, respectively. JA could get highly precise optimization results with less population size.

Acknowledgements

The authors gratefully acknowledge the financial support by the National Natural Science Foundation of China (Grant No. 51476121).

References

[1] S. Amiri, H. Shokouhmand, A. Kahrobaian, S. Amiri. Optimum flashing pressure in single and double flash geothermal power plants. ASME 2008 Heat Transfer Summer Conference collocated with the Fluids Engineering, Energy Sustainability, and 3rd Energy Nanotechnology Conferences. American Society of Mechanical Engineers2008. pp. 125-9.

[2] Y. Cerci. Performance evaluation of a single-flash geothermal power plant in Denizli, Turkey. Energy. 28 (2003) 27-35.

374 [3] N.A. Pambudi, R. Itoi, S. Jalilinasrabady, K. Jaelani. Exergy analysis and
375 optimization of Dieng single-flash geothermal power plant. Energ Convers Manage. 78
376 (2014) 405-11.
377 [4] O. Arslan. Power generation from medium temperature geothermal resources: ANN-
378 based optimization of Kalina cycle system-34. Energy. 36 (2011) 2528-34.
379 [5] W. Fu, J. Zhu, T. Li, W. Zhang, J. Li. Comparison of a Kalina cycle based cascade
380 utilization system with an existing organic Rankine cycle based geothermal power system
381 in an oilfield. Applied Thermal Engineering. 58 (2013) 224-33.
382 [6] H. Saffari, S. Sadeghi, M. Khoshzat, P. Mehregan. Thermodynamic analysis and
383 optimization of a geothermal Kalina cycle system using Artificial Bee Colony algorithm.
384 Renew Energ. 89 (2016) 154-67.
385 [7] M. Yari. Exergetic analysis of various types of geothermal power plants. Renew
386 Energ. 35 (2010) 112-21.
387 [8] L. Cao, J. Wang, P. Zhao, Y. Dai. Thermodynamic comparison among double-flash
388 flash-Kalina and flash-ORC geothermal power plants. International Journal of
389 Thermodynamics. 19 (2016) 53-60.
390 [9] J. Wang, J. Wang, Y. Dai, P. Zhao. Thermodynamic analysis and optimization of a
391 flash-binary geothermal power generation system. Geothermics. 55 (2015) 69-77.
392 [10] D.Y. Goswami, F. Xu. Analysis of a new thermodynamic cycle for combined power
393 and cooling using low and mid temperature solar collectors. Journal of Solar Energy
394 Engineering. 121 (1999) 91-7.
395 [11] F. Xu, D.Y. Goswami, S.S. Bhagwat. A combined power/cooling cycle. Energy. 25
396 (2000) 233-46.

[12] G. Demirkaya, R.V. Padilla, A. Fontalvo, M. Lake, Y.Y. Lim. Thermal and Exergetic Analysis of the Goswami Cycle Integrated with Mid-Grade Heat Sources. Entropy. 19 (2017) 416.

[13] L.C. Mendoza, D.S. Ayou, J. Navarro-Esbrí, J.C. Bruno, A. Coronas. Small capacity absorption systems for cooling and power with a scroll expander and ammonia based working fluids. Applied Thermal Engineering. 72 (2014) 258-65.

[14] H. Ghaebi, T. Parikhani, H. Rostamzadeh, B. Farhang. Proposal and assessment of a novel geothermal combined cooling and power cycle based on Kalina and ejector refrigeration cycles. Applied Thermal Engineering. 130 (2018) 767-81.

[15] W. Han, Q. Chen, L. Sun, S. Ma, T. Zhao, D. Zheng, et al. Experimental studies on a combined refrigeration/power generation system activated by low-grade heat. Energy. 74 (2014) 59-66.

[16] Y.E. Yüksel. Thermodynamic assessment of modified Organic Rankine Cycle integrated with parabolic trough collector for hydrogen production. International Journal of Hydrogen Energy. (2017).

[17] S. Khanmohammadi, P. Heidarnejad, N. Javani, H. Ganjehsarabi. Exergoeconomic analysis and multi objective optimization of a solar based integrated energy system for hydrogen production. international journal of hydrogen energy. 42 (2017) 21443-53.

[18] E. Akrami, I. Khazaee, A. Gholami. Comprehensive analysis of a multi-generation energy system by using an energy-exergy methodology for hot water, cooling, power and hydrogen production. Applied Thermal Engineering. 129 (2018) 995-1001.

418 [19] Y.E. Yuksel, M. Ozturk, I. Dincer. Thermodynamic analysis and assessment of a
419 novel integrated geothermal energy-based system for hydrogen production and storage.
420 International Journal of Hydrogen Energy. (2017).
421 [20] K. Parham, H. Alimoradiyan, M. Assadi. Energy, exergy and environmental analysis
422 of a novel combined system producing power, water and hydrogen. Energy. 134 (2017)
423 882-92.
424 [21] Z.X. Sun, J.F. Wang, Y.P. Dai, J.H. Wang. Exergy analysis and optimization of a
425 hydrogen production process by a solar-liquefied natural gas hybrid driven transcritical
426 CO2 power cycle. International Journal of Hydrogen Energy. 37 (2012) 18731-9.
427 [22] H.M. Hettiarachchi, M. Golubovic, W.M. Worek, Y. Ikegami. Optimum design
428 criteria for an organic Rankine cycle using low-temperature geothermal heat sources.
429 Energy. 32 (2007) 1698-706.
430 [23] S. Quoilin, M. Van Den Broek, S. Declaye, P. Dewallef, V. Lemort. Techno-
431 economic survey of Organic Rankine Cycle (ORC) systems. Renewable and Sustainable
432 Energy Reviews. 22 (2013) 168-86.
433 [24] D. Wei, X. Lu, Z. Lu, J. Gu. Performance analysis and optimization of organic
434 Rankine cycle (ORC) for waste heat recovery. Energ Convers Manage. 48 (2007) 1113-9.
435 [25] R.V. Rao, G. Waghmare. A new optimization algorithm for solving complex
436 constrained design optimization problems. Engineering Optimization. 49 (2017) 60-83.
437

Figure captions

448 Table 1 Simulation conditions of system

Term	Value
Environment pressure (kPa)	101.33
Environment temperature (℃)	20.00
Geothermal water temperature (℃)	170.00
Geothermal water mass flow ($kg \cdot s^{-1}$)	30.00
Pinch point temperature difference (℃)	10.00
Approach point temperature difference (℃)	7.00
Turbine isentropic efficiency (%)	75.00
Pump isentropic efficiency (%)	65.00
Mechanical efficiency (%)	96.00
Generating efficiency (%)	95.00
Pump motor efficiency (%)	95.00
Alkaline electrolyser total efficiency (%)	77.00
Flash pressure (kPa)	450.00
Steam turbine back pressure (kPa)	30.00
Ammonia mass fraction of basic solution (%)	40.00
Ammonia-water turbine inlet pressure (kPa)	2500.00
Ammonia-water turbine back pressure (kPa)	1200.00

449

450 Table 2 system performance

Term	Value
Power of steam turbine (kW)	363.56
Power of ammonia-water turbine (kW)	110.83
Power consumption of pumps (kW)	60.28
Net power output (kW)	414.10
Hydrogen production (L/s)	24.82
Refrigeration capacity (kW)	837.66
Refrigeration exergy (kW)	34.25
Ice-making capacity (kg/s)	7.25
Hydrogen production exergy efficiency (%)	18.28
System exergy efficiency (%)	20.24

451

Table 3 Operation parameters of optimization algorithm and ranges of key thermodynamic parameters

Term	Value
Population size for JA	10, 20 and 30
Population size for GA	10, 20,30, 50 and 100
Generation of optimization	100
Geothermal water temperatures, ℃	150.00, 160.00 and 170.00
Flash pressure, kPa	50.00-600.00
Steam turbine back pressure, kPa	20.00-100.00
Ammonia mass fraction of basic solution, %	20.00-99.00
Ammonia-water turbine inlet pressure, kPa	1600.00-3500.00
Ammonia-water turbine backpressure, kPa	600.00-1500.00

Table 4 Optimization results

Term / η_{exg} / t_{geo}	Population size							
	JA			GA				
	10	20	30	10	20	30	50	100
150℃	23.57%	23.59%	23.59%	18.54%	21.28%	21.11%	23.12%	23.23%
160℃	25.05%	25.06%	25.06%	13.80%	23.58%	22.44%	24.47%	24.98%
170℃	26.25%	26.25%	26.25%	18.73%	25.24%	25.49%	26.03%	26.17%

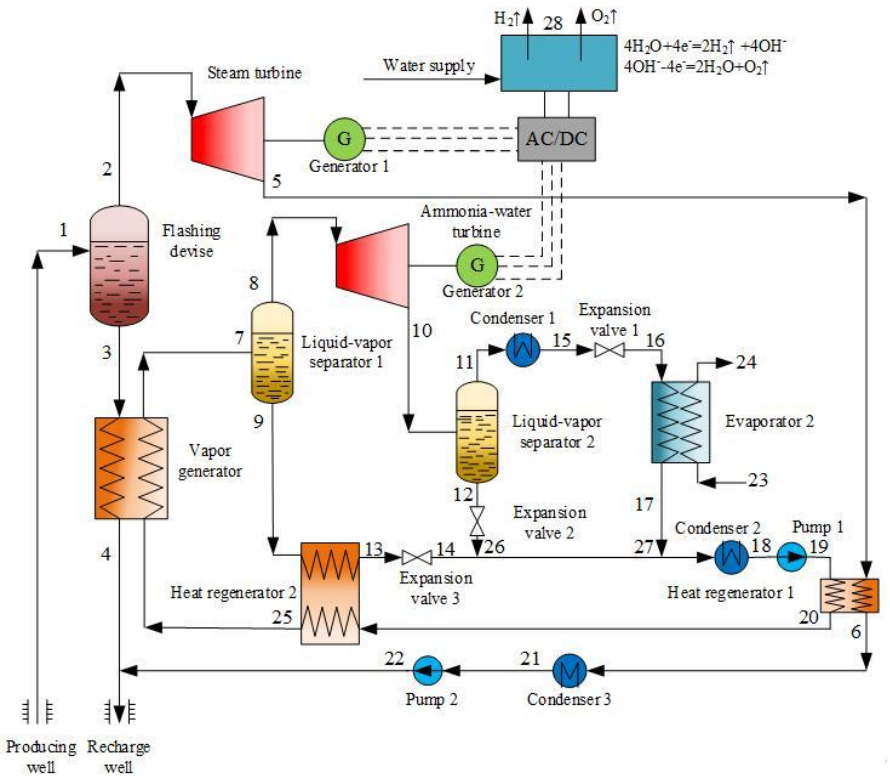

457

458 Fig. 1 The schematic diagram of a combined cooling and hydrogen production system

459

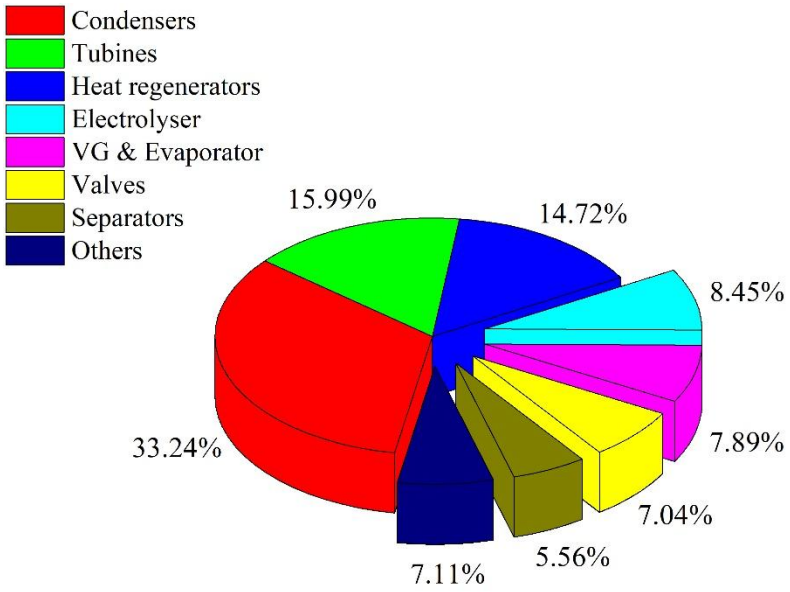

460

461 Fig. 2 Exergy destruction of different components

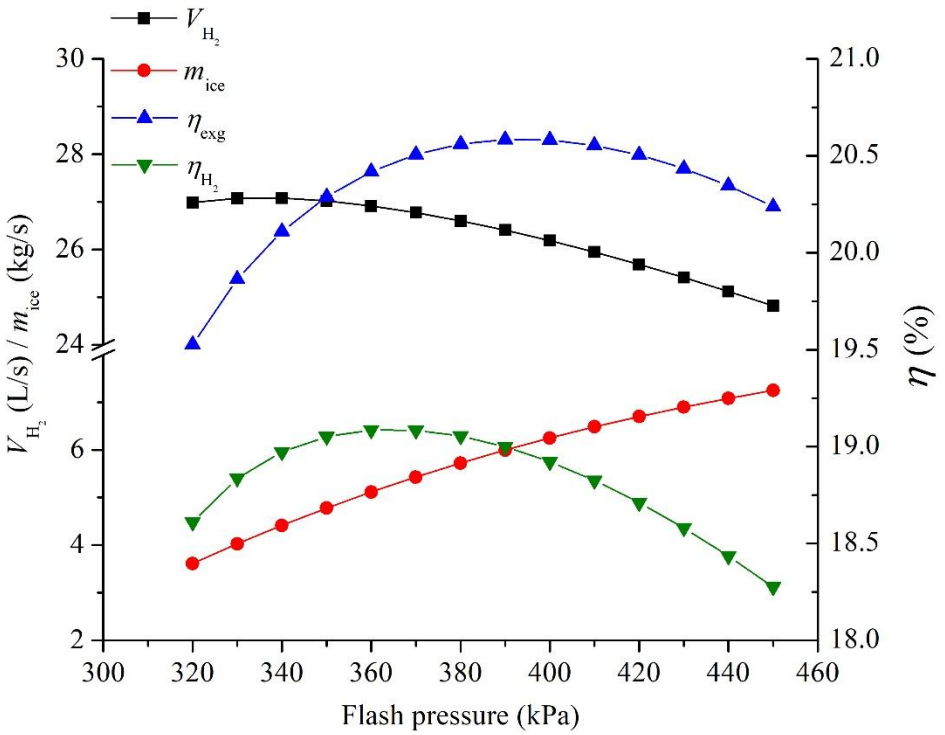

462

463 Fig. 3 The effect of flash pressure on system performance

464

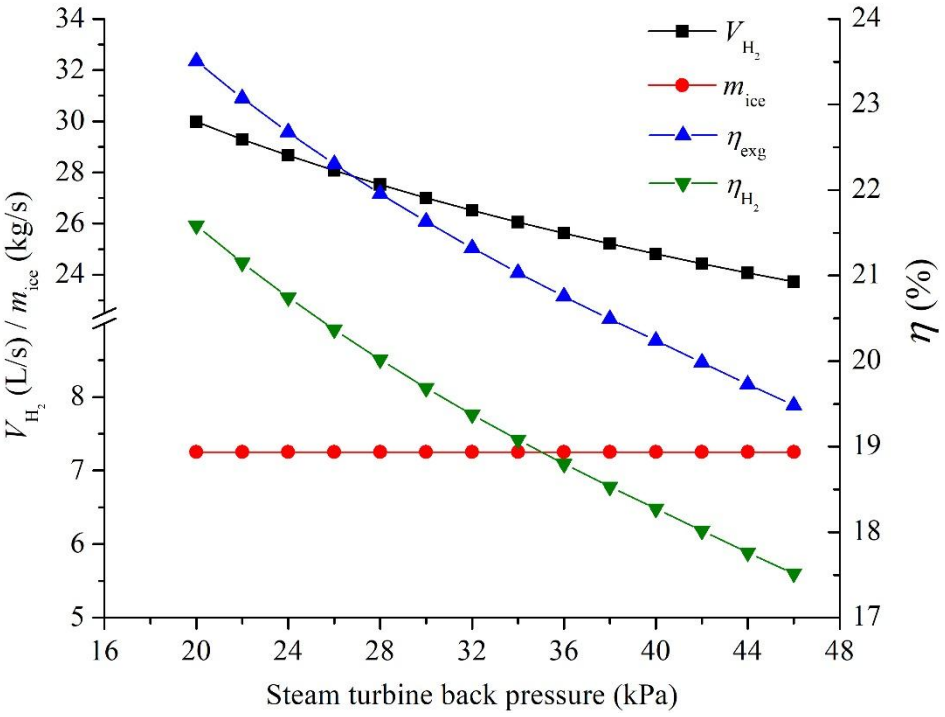

465

466 Fig. 4 The effect of steam turbine back pressure on the system performance

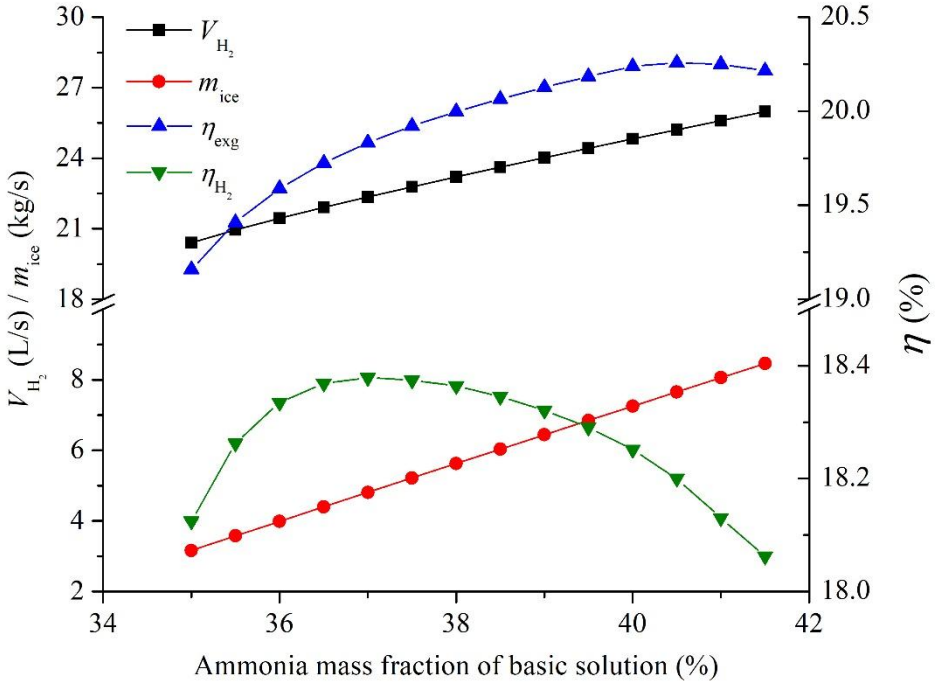

467

468 Fig. 5 The effect of ammonia mass fraction of basic solution on system performance

469

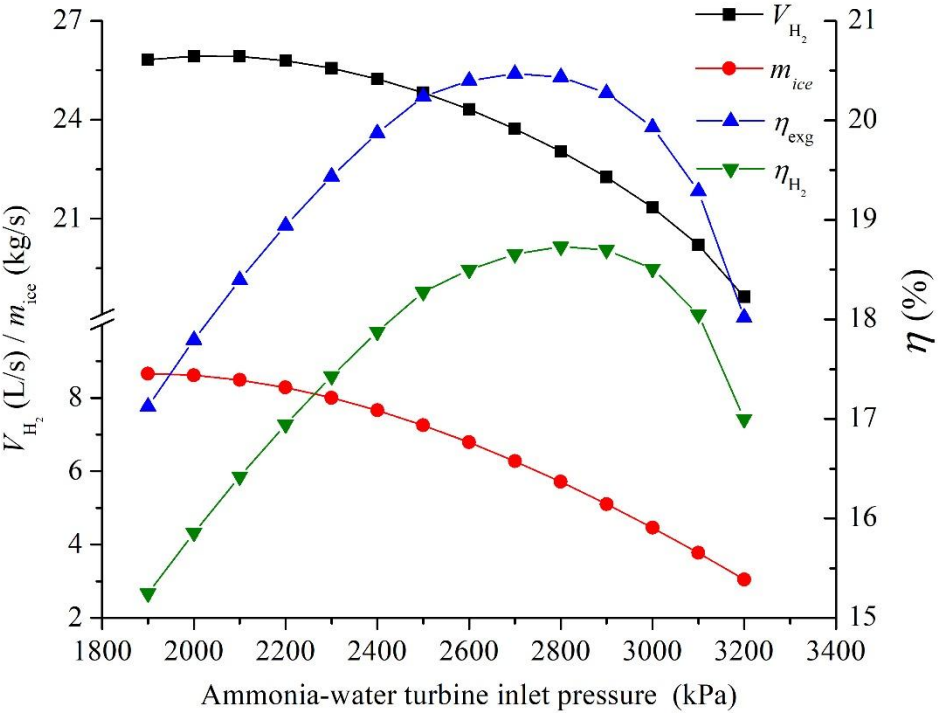

470

471 Fig. 6 The effect of ammonia-water turbine inlet pressure on system performance

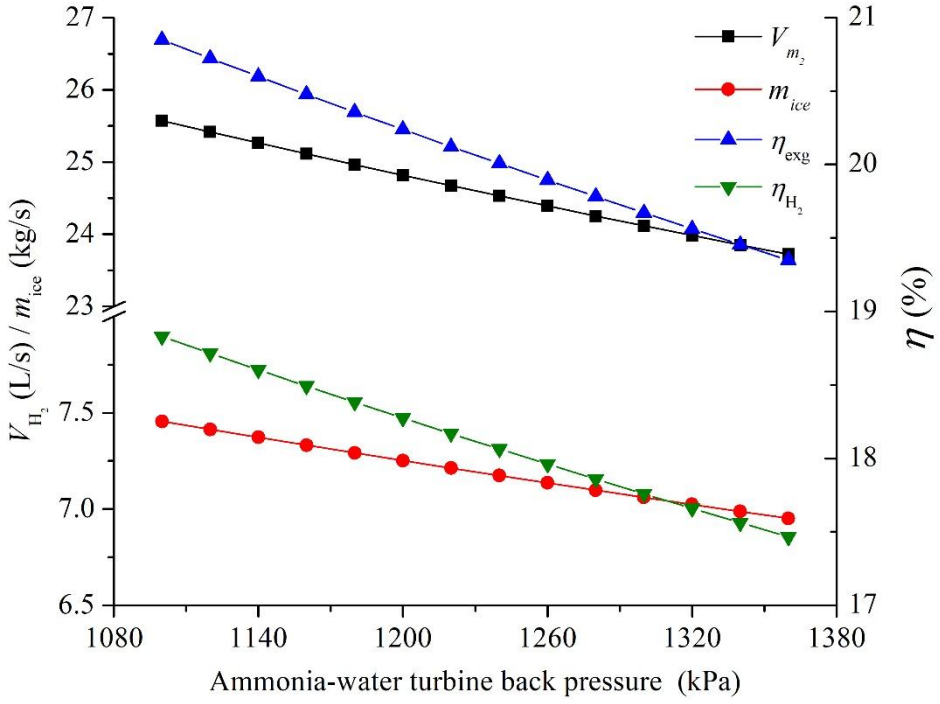

Fig. 7 The effect of ammonia-water turbine back pressure on system performance

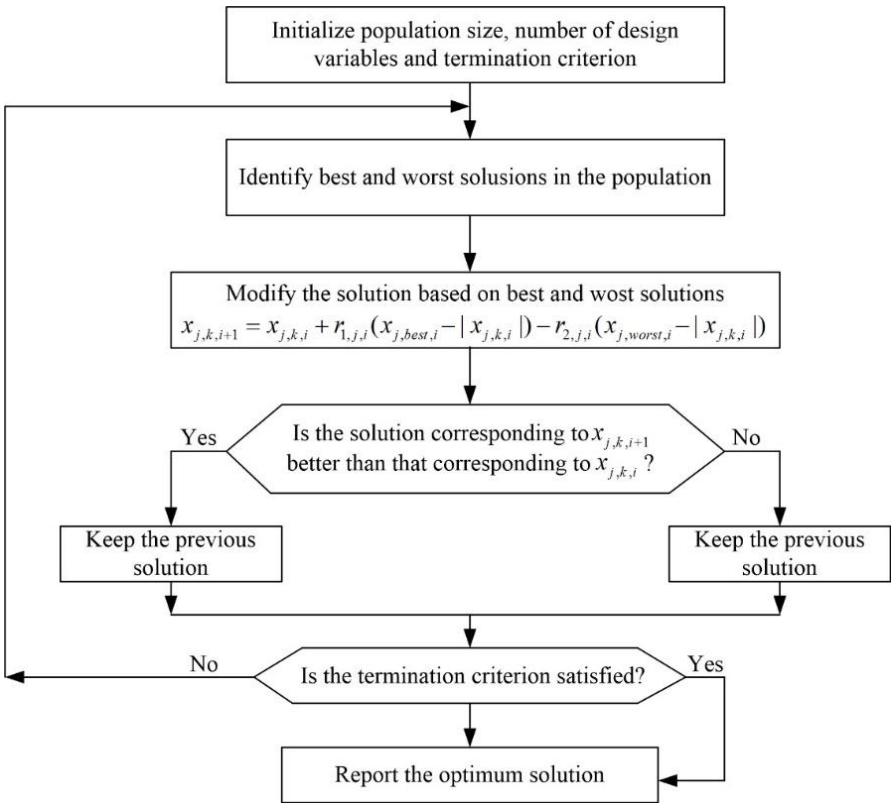

Fig. 8 The Flow chart of Jaya algorithm